

EXPERIMENTAL INVESTIGATIONS OF THE PROPAGATION OF PICOSECOND LIGHT PULSES IN SCATTERING MEDIA

K.P. Burneika, V.N. Dobrygin, G.I. Ionushauskas, A.S. Piskarskas, and V.I. Smilgyavichyus

Vilnius State University
Received January 10, 1989

This paper describes measurement techniques and experimental studies of the spatio-temporal and angular structure of narrow beams of picosecond light pulses (pulse duration $\sim t_0 \approx 10$ ps) that have passed through a finite path in a scattering medium. Pulse shape deformation, the distribution of peak intensity, and time lags for off-axis rays are discussed.

Investigations of the propagation and reflection of narrow picosecond light pulses from scattering media are of importance in connection with the problems of laser sensing of dense hydrometeorological formations, such as clouds, fogs, rains and so on. This is so because one can obtain information about such media if the duration of a pulse recorded after its interaction with a media is greater than the initial pulse duration, i.e., when $t_0 \ll \frac{1}{\epsilon V}$, where t_0 is the duration of initial pulse, ϵ is the extinction coefficient of the medium, and V is the speed of light within it¹.

In order to forecast the propagation picosecond light pulses in real scattering media, which are usually inhomogeneous, it seems to be worthwhile to carry out experiments using model media with known microphysical parameters. Thus, for example, in papers 2 and 3 an attempt has been light pulses of 20 ps duration in a water suspension of latex microspheres. In these experiments, pulse shape transformations and the time lag of the intensity peak were investigated only for paraxial beams.

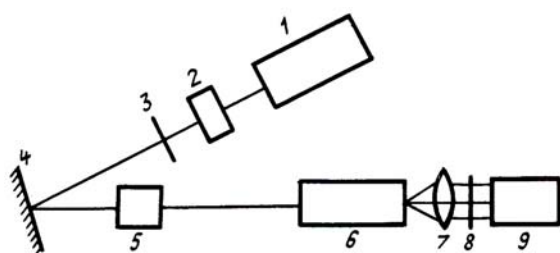


FIG 1. Block diagram of the experimental setup.

Of specific interest is the information on the spatio-temporal and angular structure of a narrow beam of picosecond light pulses passed through a scattering medium of finite length. This paper describes measurement techniques and experimental investigations of 10-picosecond pulse shape

transformations following propagation through scattering media, as well as the dependence of peak intensity and time lags on the position of the observation point transverse to the beam axis.

A block diagram of the experimental set-up is shown in Fig. 1.

The laser (1) (BeLaO₅:Nd) emits a train of 7 to 10 pulses at a wavelength of 1.07 μm . The second harmonic ($\lambda = 0.535$) was obtained using a KDP crystal (2). On the average, the duration to of a single pulse is about 10 ps. To reject spurious light at $\lambda = 1.07$ μm an SZS-21 glass absorption filter (3) was used. The second harmonic beam is directed by the mirror (4) into the beam expander (5). The collimated beam of 2 mm diameter is then directed into a cell (6) containing the scattering medium. The radiation emerging from the medium is collected with a Jupiter-9 objective (7) and directed onto the entrance slit of an Agat-SF₂ electrical image converter (9). The objective has a diameter of 42 mm and an aperture angle of about 42°. In order to increase the angular range in studies of the angular structure of scattered radiation, the entrance slit of the converter can be scanned across the image. Then, in order to match the light intensity with the linear range of the photographic film sensitivity neutral glass filters (8) were used. It was assumed in arranging the experimental setup that the optical field studied had axial symmetry around the beam axis. The scattering medium used in the experiments is a water suspension of polystyrene microspheres

with Mie parameter $\rho = 1.05$ $\left(\rho = \frac{2\pi r n_w}{\lambda} \right)$ and

refractive index $m = 1.2$. This scattering medium was assumed to be perfectly nonabsorbing, i.e., the probability of photon survival $\Lambda = 1$. The transmission of the medium was measured using a spectrophotometer. The cell, 12 mm long and 83 mm in diameter, could be filled with solutions of different optical density.

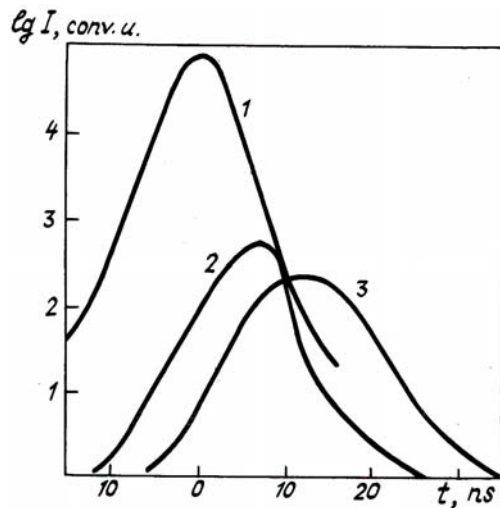


FIG. 2. Plots of the pulse shape and intensity for three scattering angles $\alpha = 0^\circ, 18^\circ, \text{ and } 28^\circ$ (curves 1, 2 and 3, respectively). Optical depth $\tau = 3.6$.

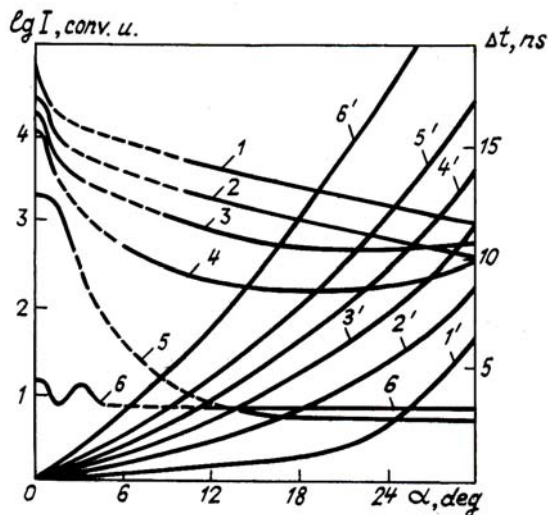


FIG. 3. Distribution of peak intensity (left ordinate) and time lag (right ordinate) over scattering angles α at different optical depths. Curves 1 and 1' are obtained with $\tau = 0.9$; 2 and 2' with $\tau = 1.35$; 3 and 3' with $\tau = 1.8$; 4 and 4' with $\tau = 3.6$; 5 and 5' with $\tau = 7.2$; and curves 6 and 6' with $\tau = 14.4$.

Figure 2 presents averaged plots of pulse shape and intensity near the beam axis for different arrival angles α . The angle α is measured between the direction of beam emergence from the end face of the sample cell and the original beam axis. Angular resolution of the measurements was 3.5° , and was determined by the size of the field stop diaphragm of the microphotometer. We used the mean value of α . The horizontal axis shows the time scale in picoseconds; the origin of this axis corresponds to the moment when the peak intensity is reached on the beam axis. The vertical axis shows the logarithm of

intensity in relative units. Optical depth of the medium in this case was $\tau = 3.6$. The value of time lags for radiation arriving at angles of 18° and 28° were $\Delta t_1 = 7$ ps and $\Delta t_2 = 14$ ps, respectively. It was also noted that to within $\delta t = \mp 2$ ps, broadening of the pulse by a factor of 1.5 to 2 took place for the radiation arriving at 28° , as compared to the duration on the beam axis, the optical depth being the same ($\tau = 3.6$). An increase in the arrival angle results in a reduction of the slope of the trailing edge, while the shape of the leading edge is practically unchanged.

Figure 3 presents the distribution of the peak intensity (curves 1 to 6) and time lag (curves 1' to 6') as functions of the arrival angle α , for different optical densities of the scattering medium. The values of the arrival angle are shown along the horizontal axis, the logarithms of the intensity are shown on the left-hand vertical axis, and the time lags for axial pulses are shown on the right-hand vertical axis. One can see from this figure that an increase in optical depth of the medium results in the diffusion of the central part of the beam due to multiple scattering. At $\tau_6 = 14.4$ (starting portion of the 6-th curve in Fig. 3), one can see the second maximum at $\alpha \approx 3$ to 4° with respect to the beam axis. This maximum can be explained by an increase in singly scattered radiation intensity at small scattering angles, with simultaneous decrease in scattering of the central part of the beam. At low optical depths ($\tau \leq 1.5$), the angular distribution of the scattered radiation is a smooth, decreasing function of angle. But for $\tau \geq 1.5$, an increase can be observed at large scattering angles (e.g. 5 to 10% at $\alpha = 28^\circ$). Dashed portions of curves 1 to 6 show the range in which the edge of the neutral-density filter affects the results. From curves 1' to 6' in Fig. 3 one can see that the time lag of peak intensity arrival increases with increasing scattering angle α . This is caused first by an increase in the geometrical path length along which scattered photons travel and second, by the time lag induced by an increase in the multiplicity of scattering.

Thus it has been shown in this paper that our technique enables one to detect shape changes in picosecond light pulses propagated through scattering media, as well as recording information on the spatio-temporal and angular structure of scattered radiation at the same time.

REFERENCES

1. A.P. Ivanov, *in: Topics in Modern Optics and Spectroscopy* (Nauka i Tekhnika, Minsk, 1980).
2. Yasuo Kuga, Akira Ishimaru, and Adam P. Bruckner, *J. Opt. Soc. Am.*, **73**, No. 12, 1812 (1983).
3. Koichi Shimizu, Akira Ishimaru, Larry Reynolds and Adam P. Bruckner, *Appl. Optics*, **18**, No. 20, 3484 (1979).